

See discussions, stats, and author profiles for this publication at: <https://www.researchgate.net/publication/5671570>

Three-Dimensional Compositional Analysis of Drug Eluting Stent Coatings Using Cluster Secondary Ion Mass Spectrometry

ARTICLE *in* ANALYTICAL CHEMISTRY · MARCH 2008

Impact Factor: 5.64 · DOI: 10.1021/ac701644j · Source: PubMed

CITATIONS

38

READS

33

3 AUTHORS, INCLUDING:



Albert Fahey

United States Naval Research Laboratory

92 PUBLICATIONS 1,938 CITATIONS

SEE PROFILE

Three-Dimensional Compositional Analysis of Drug Eluting Stent Coatings Using Cluster Secondary Ion Mass Spectrometry

Christine M. Mahoney* and Albert J. Fahey

National Institute of Standards and Technology, 100 Bureau Drive, Mail Stop 8371, Gaithersburg, Maryland 20899

Anna M. Belu

Medtronic Inc., 710 Medtronic Parkway, LT130, Minneapolis, Minnesota 55432-5604

Cluster secondary ion mass spectrometry (cluster SIMS) employing an SF_5^+ polyatomic primary ion sputter source in conjunction with a Bi_3^+ analysis source was used to obtain three-dimensional molecular information in polymeric-based drug-eluting stent coatings. The formulations of the coatings varied from 0% to 50% (w/w) sirolimus drug in poly(lactic-co-glycolic acid) and were prepared on both MP35N metal alloy coupons and bare metal stents. All cluster SIMS depth profiles obtained indicated a drug-enriched surface region, followed by a drug-depletion region, and finally a constant bulk composition region, similar to previous data obtained in polymeric blend systems. The drug overlayer thickness was determined to increase with increasing sirolimus content. Sample temperature was determined to play an important role in the resulting depth profiles, where it was shown that the best profiles were obtained at low temperatures (-100°C). At these temperatures, molecular signals typically remained constant through the entire depth of the film ($\sim 6.5\ \mu\text{m}$) in some cases, as opposed to the typical $1\ \mu\text{m}$ – $2\ \mu\text{m}$ depth limit, which is achievable at room temperature. The 3-D imaging capabilities of cluster SIMS were successfully demonstrated and indicated a significant amount of subsurface domain formation in the 25% and 50% sirolimus samples, but not in the 5% sample, which was homogeneous. These results clearly illustrate the utility of cluster SIMS for probing the 3-D structure in polymeric-based drug delivery devices.

There is much excitement and controversy in the cardiology community about cardiac stents, which are a valuable treatment for coronary artery disease. A stent is a small, coiled, wire-mesh tube that is inserted permanently into an artery during an angioplasty procedure. The stent acts as a scaffold, helping to keep the artery open and decrease the probability of restenosis of the artery (buildup of smooth muscle cells at the site of the stent). To further prevent restenosis, some stents have incorporated a drug delivery system into the structure of the stent, where a drug (e.g., paclitaxel or sirolimus) is released at a controlled rate from

a polymer film or multiple polymeric layers. This drug serves to prevent cell regrowth from blocking the artery again at the angioplasty site.^{1–3}

As compared to bare metal stents (BMS), drug-eluting stents (DES) decrease the rate of restenosis by as much as 30%.⁴ Though there are decreases in the occurrence of restenosis, there may be long-term complications resulting from increased occurrences of thrombosis or clotting of the artery when using DES as compared to those using BMS.⁴ Therefore, it is also necessary that the biomaterials selected for delivery be biocompatible and antithrombotic.

Finally, like every other drug delivery device, it is important that the drug is delivered in a controlled manner to optimize the performance and minimize the toxicity of the drug. It is particularly important to fully characterize the molecular composition of the surface and near-surface region of the device (outer 500 nm) because this region controls the biocompatibility and influences the magnitude and temporal variation of drug release. Dissolution studies are typically used to monitor the rate of drug release. However, these studies need to be correlated with actual structural information, compositions, and defects within the device. With recent advancements in secondary ion mass Spectrometry (SIMS), this is now possible.

SIMS is a mass spectrometric-based analytical technique that provides information about the molecular, elemental, and isotopic composition of a surface. In a conventional SIMS experiment, an energetic primary ion beam, such as Ga^+ , Cs^+ , or Ar^+ , is focused onto the sample surface. The interaction of this beam with the sample results in the desorption of secondary ions from the surface of the material, which are then extracted into a mass spectrometer. Widespread use of SIMS for imaging and depth profiling of organic systems has historically been limited by low secondary ion yields and beam-induced damage effects. One potential solution to this limitation is to use cluster or polyatomic

- (1) Van der Hoeven, B. L.; Pires, N. M. M.; Warda, H. M.; Oemrawsingh, P. V.; van Vlijmen, B. J. M.; Quax, P. H. A.; Schali, M. J.; van der Wall, E. E.; Jukema, W. *Int. J. Cardiol.* **2005**, *99*, 9–17.
- (2) Dogrell, S. A. *Expert Opin. Pharmacother.* **2004**, *5* (11), 2209–2220.
- (3) Ellis, J. T.; Kilpatrick, D. L.; Consigny, P.; Prabhu, S.; Hossainy, S. F. A. *Crit. Rev. Ther. Drug Carr. Syst.* **2004**, *22* (1), 1–25.
- (4) Luscher, T. F.; Steffel, J.; Eberli, F. R.; Joner, M.; Nakazawa, G.; Tanner, F. C.; Virmani, R. *Circulation* **2007**, *115*, 1051–1058.

* To whom correspondence should be addressed. E-mail: cmahoney@nist.gov.

primary ion beams. With the application of cluster primary ion sources, such as C_{60}^+ , C_8^- , Au_3^+ , SF_5^+ , and more recently Bi_3^+ , one typically achieves significant improvements in characteristic molecular secondary ion yields (greater than 1000-fold in some cases) and also decreased beam-induced sample damage in organic and polymeric materials.^{5–8} The reduction in beam damage allows for molecular depth profiling of organic and polymeric materials with depth resolutions as low as 5 nm–10 nm.^{5,9–17} This capability for in-depth analysis would have been unheard of less than a decade ago, when these instruments employed conventional atomic sources.

Cluster SIMS has already proven to be a useful tool in the analysis of various drug delivery systems.^{9,13–16,18} With cluster SIMS, the distribution of both drugs and excipients within a drug delivery system can be determined with a high degree of spatial resolution (100 nm–500 nm), sensitivity (as low as $\mu\text{g/g}$ (ppm)), and depth resolution (5 nm–10 nm) when compared to other analytical methods such as Raman and IR spectroscopies. It is an ideal tool, in particular for the characterization polymeric-based drug delivery devices, such as DES, as many of these materials have already been proven to be amenable to in-depth analysis using this technique.^{9,12,13}

Earlier work has demonstrated the feasibility of using SIMS for characterization of drug-eluting stent materials.^{13,14,19} The earliest of these works, by Verhoeven et al., describes a method for in-depth stent characterization using conventional SIMS, where an oxygen beam is used to obtain elemental information as a function of depth in an actual stent coating.¹⁹ This work employed a more conventional oxygen beam, which does extensive damage to the sample, precluding the ability to obtain molecular information about the sample as a function of depth. Mahoney et al. described depth profiling in various polymeric-based model systems using SF_5^+ cluster beams, where the films are extremely thin (~ 200 nm) as compared to what is typically observed in the real world (up to 10 μm).¹³ Finally, Braun et al. used C_{60}^+ to depth profile through a thicker poly(styrene-*co*-isobutylene)/paclitaxel-based model system.¹⁴ None of these studies demonstrates the capability to image the composition as a function of depth.

In the current work, we report the first example of 3-D molecular profiling in a DES system using dual beam cluster SIMS (SF_5^+ ions for sputtering and Bi_3^+ ions for analysis) at low temperatures. This work will demonstrate that it is feasible to use certain cluster sources for 3-D characterization in polymeric-based drug delivery devices and that it is an ideal tool for predicting, optimizing, and verifying the performance characteristics in many drug delivery devices, including DES systems.

EXPERIMENTAL SECTION

Sample Preparation. Solutions were prepared by dissolving varying amounts of sirolimus (ZYP Pharm Chemical, Shanghai, China) and poly(DL-lactide-*co*-glycolide) (PLGA) with 50:50 lactide/glycolide (Sigma, St. Louis, MO) into a chloroform solution. These solutions (1.5% w/w in chloroform) were then cast onto metal alloy (MP35N) coupons, resulting in thick films ($6.0 \mu\text{m} \pm 0.6 \mu\text{m}$) of PLGA containing 0%, 5%, 25%, and 50% (w/w) sirolimus. Similar solutions (1% w/w in chloroform) were spray coated onto bare metal stents made of MP35N. The stents were 18 mm in length with cylindrical struts of $\sim 80 \mu\text{m}$ in diameter. The outer diameter coating thickness was measured to be $\sim 6 \mu\text{m}$ by interferometry. In one case, a pure PLGA cap coat was created by spray coating the polymer on a 25% sirolimus layer on a stent. The coating with the cap coat was prepared so that the drug/polymer layer was $\sim 3.5 \mu\text{m}$ and the cap coat was $\sim 3.5 \mu\text{m}$.

Stents were prepped for SIMS analysis by cutting them longitudinally and opening them up with tweezers. The stent was then pressed into multiple layers of indium foil with the outer diameter facing outward. For more information on these stent films, see ref 20.

Solutions (1% w/w in chloroform) were also spun cast onto Si wafers for sputter rate determinations with a resulting average film thickness of $200 \text{ nm} \pm 14 \text{ nm}$.

Time-of-Flight Secondary Ion Mass Spectrometry (TOF-SIMS). TOF-SIMS experiments were performed on an Ion-TOF IV (Münster, Germany) instrument equipped with both Bi (Bi_n^+ , where $n = 1–7$) and SF_5^+ primary ion beam cluster sources.²¹ Sputter depth profiling was performed in the dual-beam mode (two different primary ion guns were used: one for collecting spectra and one for sputtering). The analysis source was a pulsed, 25-keV bismuth cluster ion source (Bi_3^+), which bombarded the surface at an incident angle of 45° to the surface normal. The target current was maintained at $\sim 0.3 \text{ pA}$ ($\pm 10\%$) pulsed current with a raster size of $200 \mu\text{m} \times 200 \mu\text{m}$ for all experiments. Both positive and negative secondary ions were extracted from the sample into a reflectron-type time-of-flight mass spectrometer. The secondary ions were then detected by a microchannel plate detector with a postacceleration energy of 10 kV. A low-energy electron flood gun was utilized for charge neutralization in the analysis mode.

The sputter source used was a 5-keV SF_5^+ cluster source also operated at an incident angle of 45° to the surface normal. The

- (5) Stapel, D.; Thiemann, M.; Benninghoven, A. *Appl. Surf. Sci.* **2000**, *158*, 362–374.
- (6) Gillen, G.; Roberson, S. *Rapid Commun. Mass Spectrom.* **1998**, *12*, 1303–1312.
- (7) Weibel, D.; Wong, S.; Lockyer, N.; Blenkinsopp, P.; Hill, R.; Vickerman, J. C. *Anal. Chem.* **2003**, *75*, 1754–1764.
- (8) Kollmer, F. *Appl. Surf. Sci.* **2004**, *231–232*, 153–158.
- (9) Brox, O.; Hellweg, S.; Benninghoven, A. *Int. Conf. Secondary Ion Mass Spectrom.* **2000**, *12*, 777–780.
- (10) Wucher, A. *Appl. Surf. Sci.* **2006**, *252*, 6482–6489.
- (11) Cheng, J.; Winograd, N. *Appl. Surf. Sci.* **2006**, *252*, 6498–6501.
- (12) Mahoney, C. M.; Roberson, S. V.; Gillen, G. *Anal. Chem.* **2004**, *76*, 3199–3207.
- (13) Mahoney, C. M.; Patwardhan, D. V.; McDermott, M. K. *Appl. Surf. Sci.* **2006**, *19*, 6554–6557.
- (14) Braun, M.; R.; Cheng, J.; Parsonage, E. E.; Moeller, J.; Winograd, N. *Anal. Chem.* **2006**, *78* (24), 8347–8353.
- (15) Mahoney, C. M.; Yu, J. X.; Gardella, J. A., Jr. *Anal. Chem.* **2005**, *77* (11), 3570–3578.
- (16) Mahoney, C. M.; Yu, J.-X.; Fahey, A. J.; Gardella, J. A., Jr. *Appl. Surf. Sci.* **2006**, *252*, 6609–6614.
- (17) Wagner, M. S. *Anal. Chem.* **2004**, *76*, 1264–1272.
- (18) Belu, A. M.; Davies, M. C.; Newton, J. M. Patel, N. *Anal. Chem.* **2000**, *72*, 5625–5638.
- (19) Verhoeven, M. L. P. M.; Driessen, A. A. G.; Paul, A. J.; Brown, A.; Canry, J.-C.; Hendriks, M. J. *J. Controlled Release* **2004**, *96*, 113–121.

- (20) Belu, A. M.; Mahoney, C. M.; Wormuth, K. Chemical Imaging of Drug Eluting Coatings: TOF-SIMS Depth Profiling and Confocal Raman Microscopy. *J. Controlled Release*, accepted for publication.

- (21) Certain commercial equipment, instruments, or materials are identified in this article to specify adequately the experimental procedure. Such identification does not imply recommendation or endorsement by the National Institute of Standards and Technology, nor does it imply that the materials or equipment identified are necessarily the best available for the purpose.

operating conditions of the source varied with sample type (e.g., thin films on Si, thick films on the MP35N alloy, or thick films on stents). For thin model films on Si, the SF_5^+ current was maintained at ~ 2.7 nA with a $750\ \mu\text{m} \times 750\ \mu\text{m}$ raster. For the thick films on coupons and for the films on stents, the current was maintained at ~ 6 nA with a $500\ \mu\text{m} \times 500\ \mu\text{m}$ raster in order to remove the material at a faster rate. All of these SF_5^+ ion doses are well above the static SIMS limit and thus can be considered dynamic SIMS (significant damage and/or removal of material is occurring). All primary beam currents were measured with a Faraday cup both prior to and after depth profiling.

All depth profiles were acquired in the noninterlaced mode with a 5-ms pause between sputtering and analysis. Each spectrum was averaged over a 7.37-s time period (3 complete scans at 128×128 pixels). These conditions resulted in Bi_3^+ ion doses that were well below the static SIMS limit of 10^{13} ions/cm². The analysis was immediately followed by 15 s of SF_5^+ sputtering. For depth profiles of the surface and subsurface regions only, the sputter time was decreased to 1 s for the 5% sirolimus sample and 2 s for both the 25% and 50% sirolimus samples in order to allow for increased data density in this region. Depth profiles were also acquired using a Ga^+ source operated under conditions similar to that of the Bi_3^+ source, with the following exceptions: (1) the Ga was operated at ~ 2 -pA pulsed current, (2) the analysis time was 5 s per data point, and (3) the SF_5^+ sputter interval was 10 s. Images displayed in this work were reconstructed from the raw data.

Temperature-controlled depth profiles were obtained using a variable-temperature stage with a Eurotherm Controls (Worthing, UK) temperature controller and IPSPG V3.08 software. Samples were first placed into the analysis chamber at room temperature. The sample was brought to the desired temperature under ultrahigh-vacuum conditions and was allowed to stabilize for 1 min prior to analysis. All depth profiling experiments were performed both at $-100\ ^\circ\text{C}$ and $25\ ^\circ\text{C}$.

Sputter rates for all materials were determined by dividing the thickness of the model films by the time required to sputter through the films (time where the intensity of Si is 50% of its maximum value). Sputter rates can be reported as nanometers per second or volume removed per incident SF_5^+ primary ion ($\text{nm}^3/\text{SF}_5^+$). The following average sputter rates were calculated based on depth profiling in the thin films at $-100\ ^\circ\text{C}$ and $25\ ^\circ\text{C}$: (a) $(29.9 \pm 2.0)\ \text{nm}^3/\text{SF}_5^+$ for 5% sirolimus, (b) $(36.1 \pm 3.2)\ \text{nm}^3/\text{SF}_5^+$ for 25% sirolimus, and (c) $(33.0 \pm 0.1)\ \text{nm}^3/\text{SF}_5^+$ for 50% sirolimus. Pure PLGA solutions for model film preparation were not provided, but the sputter rates are assumed to be similar as determined for the other compositions ($\sim 33\ \text{nm}^3/\text{SF}_5^+$). Film thickness measurements were made by stylus profilometry (Tencor Instruments alpha-step 200, Milpitas, CA) with a 10-mg stylus force. All film thicknesses reported are average values based on five separate measurements.

RESULTS AND DISCUSSION

Thin Model Films on Si. Initial studies were performed on thin PLGA/sirolimus model films (~ 200 nm) spun cast onto Si substrates. This was done in order to (1) establish feasibility of in-depth characterization of these materials using this approach, (2) determine ideal operating conditions, (3) obtain reference spectra, and (4) determine sputter rates. Figures 1 and 2 depict

positive secondary ion mass spectra of both PLGA and sirolimus model films, respectively. The mass spectra of PLGA depicted in Figure 1 is consistent with earlier work.^{11,13,22,23,24} Figure 2 depicts the mass spectra of the sirolimus. As can be seen here, there is a significant amount of surface contamination from a commonly observed surface contaminant, poly(dimethylsiloxane) (PDMS).²⁵ These peaks are colored in blue. The peaks emphasized in red represent the ions that were selected for characterization as a function of depth. These peaks were selected because they are typically the most intense peaks in the spectra and remain so with increasing dose. It should be noted, however, that raw data were collected, meaning that the entire mass spectrum has been monitored as a function of depth or SF_5^+ ion dose. From these data, it can be seen that other than an initial change in relative intensities in the static regime (doses of up to $\sim 1 \times 10^{13}$ ions/cm² SF_5^+), all secondary ions that are characteristic of sirolimus will follow the same trend as $m/z = 84$. Similarly, all secondary ions that are characteristic of PLGA will follow the same trend as $m/z = 56$ or $m/z = 99$.

Figure 3a shows a representative depth profile, which plots the intensities of selected secondary ions as a function of increasing SF_5^+ dose (number of SF_5^+ ions impacting the surface per cm²—directly related to depth), acquired at $-100\ ^\circ\text{C}$, from the most concentrated sample (50% sirolimus in PLGA). The selected ions plotted are characteristic secondary ions signals for silicon ($m/z = 28$, Si^+), PLGA ($m/z = 56$, $\text{C}_3\text{H}_4\text{O}^+$), and sirolimus ($m/z = 84$, $\text{C}_5\text{NH}_{10}^+$).

In this particular system, the drug tends to migrate to the surface, creating a diffusion profile in the subsurface region. This diffusion profile is defined by a surface-enriched drug region, followed by a drug-depleted region, a constant bulk composition region, and finally a second interfacial region (DES film/Si interface), which in this case shows a drug-enriched Si interface undergoing diffusion characteristics similar to those observed at the surface. This type of diffusion profile is consistent with that observed in previous work with polymeric blend systems, but is much more noticeable due to the increased secondary ion yields obtained with the Bi cluster source (previous work used Ar^+).^{15,16}

Note that the profile in Figure 3a was acquired at $-100\ ^\circ\text{C}$. Earlier work describing the effects of temperature on polymeric depth profiling indicated that temperature plays an important role in polymeric depth profiling and should be considered when optimizing depth profiling conditions.^{13,26–29} The overall results indicated that, for poly(methyl methacrylate), there was decreased sputter-induced topography formation resulting from more uniform sputtering at low temperatures. It was suggested that at low

(22) Boschmans, B.; Van Royan, P.; Van Vaeck, L. *Rapid Commun. Mass Spectrom.* **2005**, *19*, 2517–2527.

(23) Davies, M. C.; Short, R. D.; Khan, M. A.; Watts, J. F.; Brown, A.; Eccles, A. J.; Humphrey, P.; Vickerman, J. C.; Vert, M. *Surf. Int. Anal.* **1989**, *14*, 115–120.

(24) Shard, A. G.; Volland, C.; Davies, M. C.; Kissel, T. *Macromolecules* **1996**, *29*, 748–754.

(25) Cherian, J. T.; Castner, D. G. *J. Adv. Mater.* **2000**, *32* (1), 28–33.

(26) Mahoney, C. M.; Fahey, A. J.; Gillen, G. *Anal. Chem.* **2007**, *79* (3), 828–836.

(27) Mahoney, C. M.; Fahey, A. J.; Gillen, G.; Xu, C.; Batteas, J. D. *Anal. Chem.* **2007**, *79* (3), 837–845.

(28) Mahoney, C. M.; Fahey, A. J.; Gillen, G.; Xu, C.; Batteas, J. D. *Appl. Surf. Sci.* **2006**, *19*, 6502–6505.

(29) Mollers, R.; Ruccitto, N.; Torrisi, V.; Niehuis, E.; Licciardello, A. *Appl. Surf. Sci.* **2006**, *252*, 6509–6512.

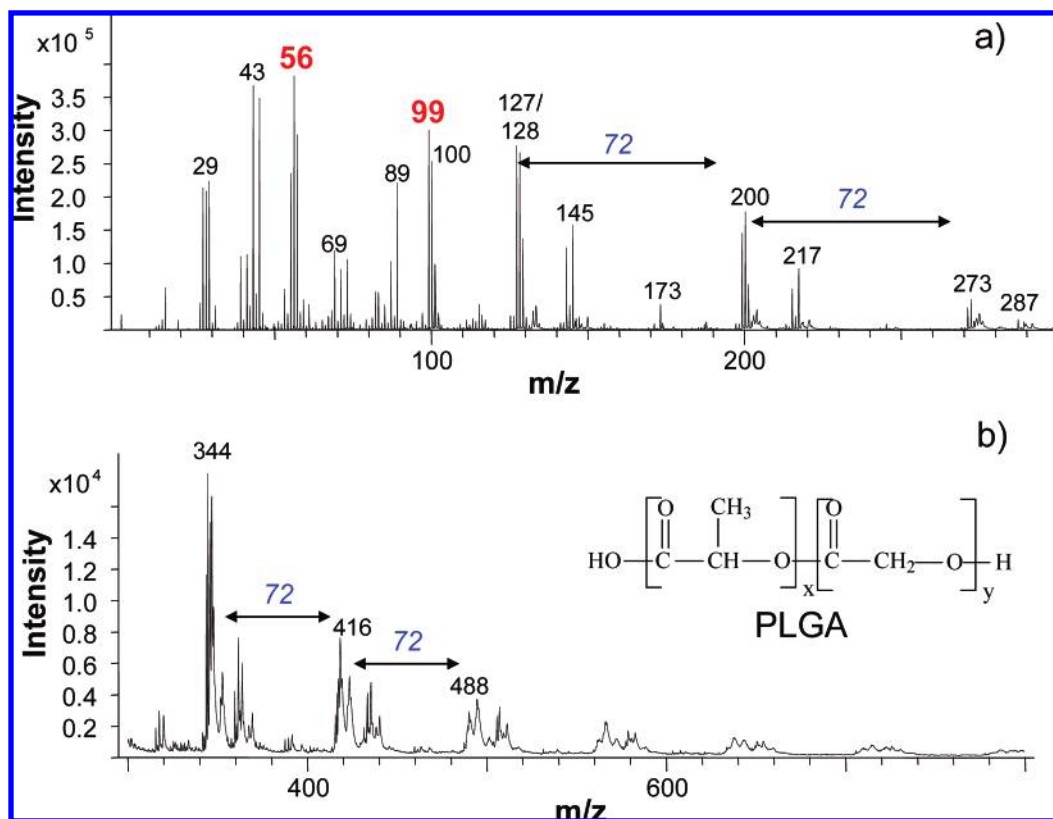


Figure 1. Positive secondary ion mass spectra acquired from a PLGA film spun cast on Si: (a) $m/z = 0$ to $m/z = 300$ and (b) $m/z = 300$ to $m/z = 800$. Peaks labeled with boldface red letters were selected for 3-D analysis. Note that the major peaks are separated by $m/z = 72$, the mass of the polymeric repeat unit in poly(lactic acid) (PLA).

temperatures the polymer properties changed considerably, thereby changing the chemical and physical interaction of the SF_5^+ beam with the sample. It is also possible that the extent of cross-linking is decreased at low temperatures. The importance of temperature is also evident in this system when comparing Figure 1a and b acquired at -100°C and 25°C , respectively. In Figure 3a, the profile shows very distinct features, sharp interfaces, and high Si intensities at the interface, whereas in Figure 3b, the signal decays with increasing sputtering, the polymer/Si interface is broadened significantly, and the intensity of the Si at the interface is very low. These results indicate that temperature will play an important role in depth profiling in thicker films as well.

Similar profiles were obtained from the 5% and 25% samples at varying temperatures. In general, the quality of the profiles obtained at room temperature decreased with increasing sirolimus content (increased signal decay, broadened interface widths, low substrate signals, etc.). This effect of decreasing depth profile stability at high drug concentrations has been observed previously in PLA/acetaminophen model systems.¹¹ It is assumed that the presence of the drug induces inhomogeneities in the film, which increase topography formation and damage accumulation. Because of this, the temperature effects were not as obvious for the 5% sample as for the 25% and 50% samples. However, all compositions showed some form of improvement at low temperatures, with the most prevalent effect being decreased interface widths.

Thick Films on MP35N Alloy Coupons. The high-quality profiles (intense signals, sharp interface widths, etc.) depicted in Figure 3 are not surprising because PLGA and other polyesters have already proven to be the most successful depth profiles to

date and are extremely amenable to polyatomic primary ion bombardment.^{12,13,15,16} However, when employing an SF_5^+ source at room temperature, the information obtained is typically limited to the top $1\ \mu\text{m}$ – $2\ \mu\text{m}$ for PLGA, after which a complete loss of secondary ion signal will be observed, indicative of significant damage accumulation. This damage accumulation is much worse in other types of polymeric materials, where the signal loss typically occurs after depth profiling through $\sim 150\ \text{nm}$ – $200\ \text{nm}$ of material.³⁰ In real-world samples, however, the thickness of films is often much greater than this. Drug-eluting stent coatings, for example, usually have thicknesses of up to $10\ \mu\text{m}$. Therefore, we expected this technique to be limited to the surface and subsurface regions.

Figure 4 depicts representative depth profiles acquired from thick DES coatings ($6\ \mu\text{m}$) cast on an MP35N alloy coupon, where the depth profiles shown here are from both the PLGA control film and the 50% sirolimus film acquired at different temperatures. The selected ion intensities were characteristic of the PLGA ($m/z = 56$), the alloy substrate ($m/z = 52$, Cr^+), and PDMS ($m/z = 73$, $\text{Si}(\text{CH}_3)^+$).^{12,15,22–24} The profile of the pure PLGA control film, with no drug added, is shown in Figure 4a. Here the signal intensities drop at an ion dose of $\sim 1 \times 10^{15}$ ions/ cm^2 . Note that the interface is never reached, as the signal for Cr^+ remains low through the entire profile. After lowering the temperature to -100°C during the profile acquisition; however, the depth profile stability improves considerably. Though there is a slight decrease

(30) Note that these values are reported specifically for SF_5^+ and may not be consistent with what is observed using other cluster ion sources, such as C_{60}^+ .

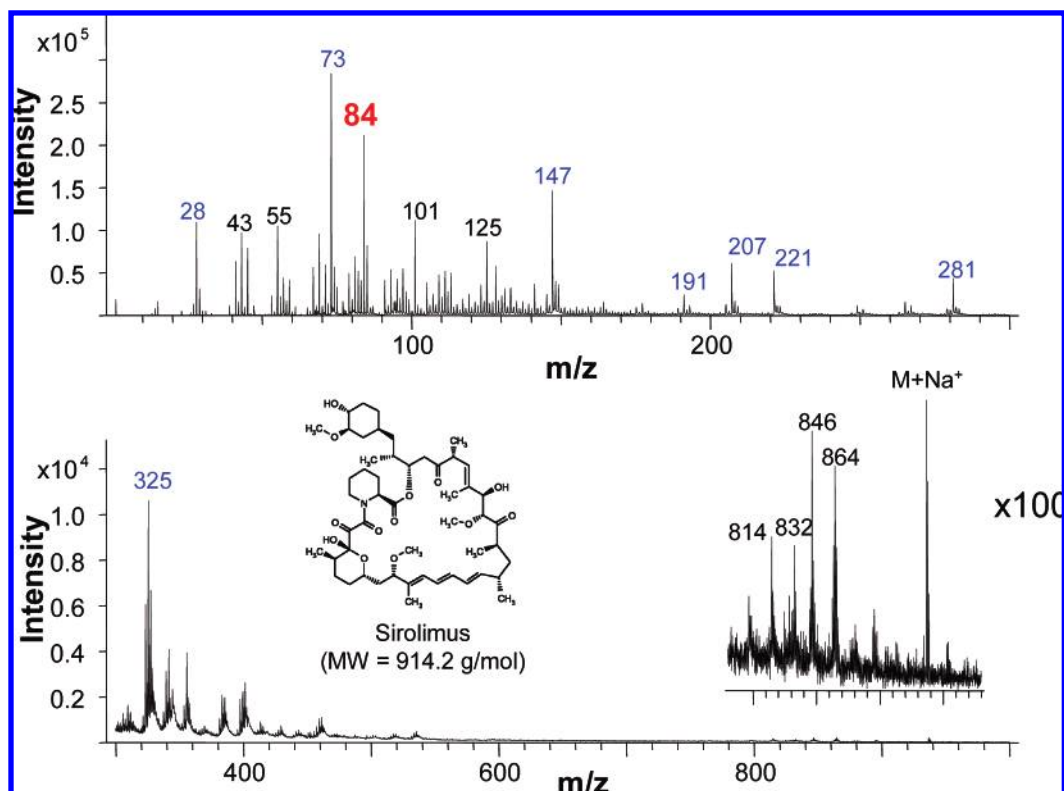


Figure 2. Positive secondary ion mass spectra of sirolimus cast onto Si wafer: (a) m/z = 0 to m/z = 300 and (b) m/z = 300 to m/z = 1000. Peaks labeled in blue represent PDMS contamination. Peaks labeled in boldface red letters were selected for 3-D analysis.

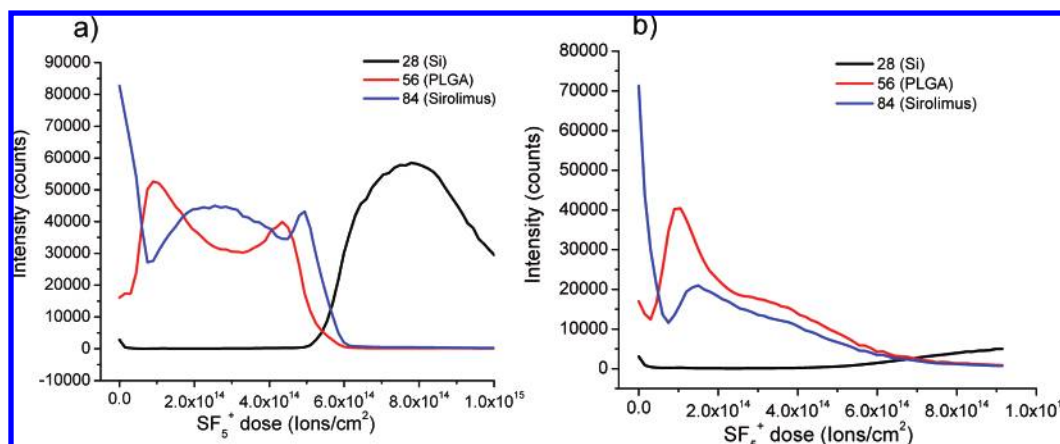


Figure 3. Selected secondary ion intensities plotted as a function of SF_5^+ dose in a PLGA film (201 ± 18 nm) containing 50% sirolimus. Data were acquired using a Bi_3^+ analysis source and an SF_5^+ sputter source: (a) acquired at $-100^\circ C$ and (b) acquired at $25^\circ C$.

in signal intensity after $\sim 6 \times 10^{15}$ ions/cm², the signal remains high, up through to the interfacial region, which is located at $\sim 1.7 \times 10^{16}$ ions/cm². At this point, an increase in the substrate signal (m/z = 52) is observed in correspondence with loss of all molecular signal characteristic of the film. This result further illustrates the importance of temperature-controlled depth profiling of polymeric based films, as $6 \mu m$ is a much thicker polymeric film than has been achieved before with this type of system. The average crater depths of the samples sputtered at room temperature were determined to be $2.1 \mu m \pm 0.4 \mu m$ thick as opposed to the $6.0 \mu m \pm 0.6 \mu m$ thick crater bottoms achieved at low temperatures. It is assumed that, similar to previous work, there is decreased sputter-induced topography formation and decreased damage accumulation at low temperatures, resulting from an

increased uniformity of sputtering.²⁷ This allows one to maintain signals for much longer periods of time. The slight decrease in signal intensity at $\sim 6 \times 10^{15}$ ions/cm² (Figure 4b) was not seen consistently and is thought to be some sort of charging effect resulting from poor film quality (films were very rough).

The same experiments were performed on the 5%, 25%, and 50% sirolimus samples, where it was determined that profiling through the entire film could also be achieved in the 5% sirolimus samples. However, with higher concentrations, profiling through the entire film proved difficult. It is assumed that the presence of the drug induces increased topography formation and damage accumulation and therefore results in loss of signal at an earlier time during the profile process. The results from the 50% sirolimus sample are shown in panels c and d in Figure 4, which depict

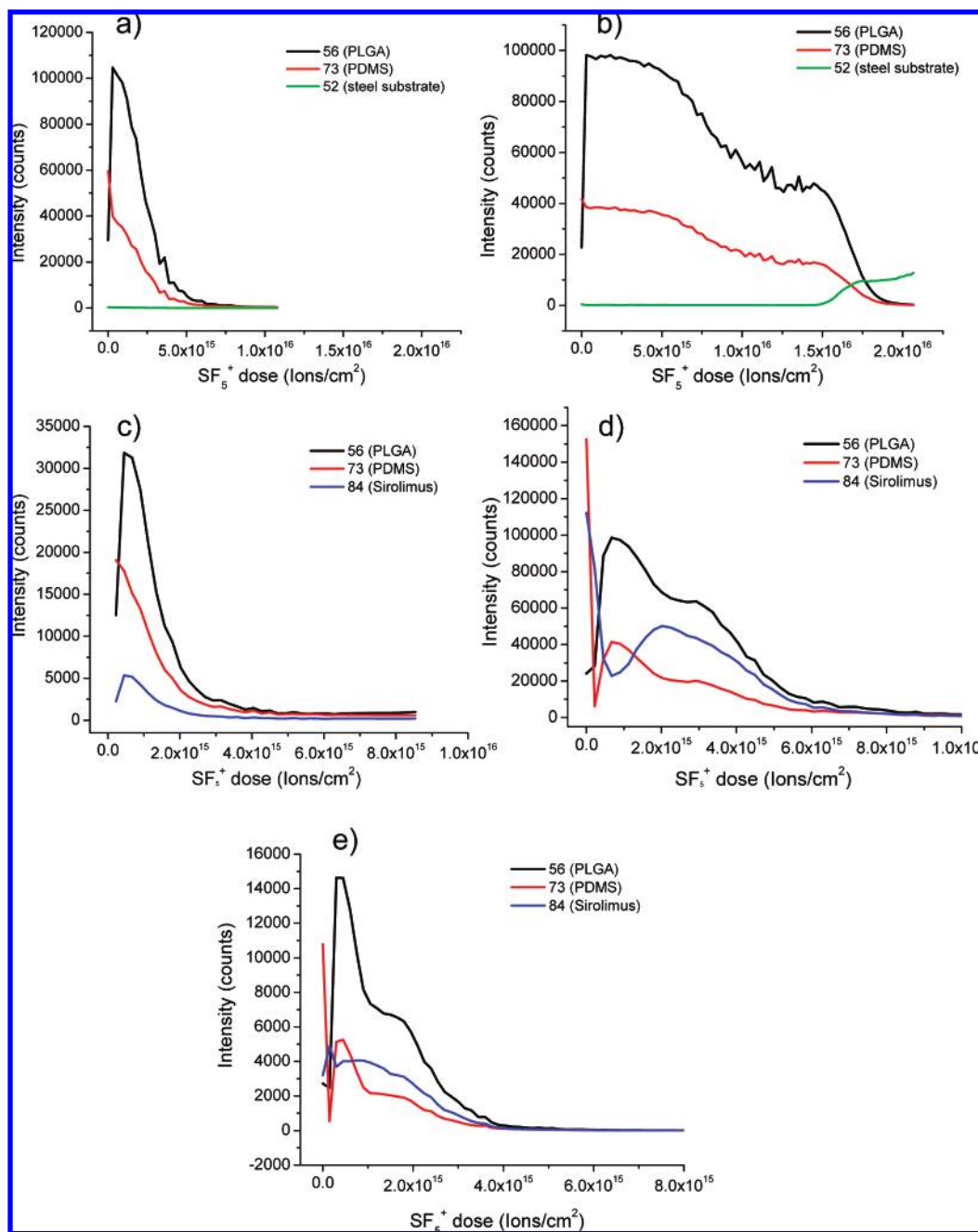


Figure 4. Selected secondary ion intensities plotted as a function of SF_5^+ dose (directly related to depth). Data were acquired using a Bi_3^+ analysis source and an SF_5^+ sputter source: (a) PLGA film, acquired at 25 °C, (b) PLGA film, acquired at -100 °C, (c) 50% sirolimus in PLGA, acquired at 25 °C, (d) 50% sirolimus in PLGA, acquired at -100 °C, and (e) 50% sirolimus in PLGA, acquired at -100 °C (Ga^+ primary ion source for analysis).

profiles acquired at 25 °C and -100 °C, respectively. Although the substrate was not reached with these more concentrated samples, the benefits of low-temperature analysis can clearly be seen. Very little useful information can be obtained from the 50% sirolimus sample acquired at room temperature (see Figure 4c), as the signal decays rather quickly ($<7 \times 10^{14} SF_5^+$ ions/cm² with corresponding crater depths of ~500 nm). However, in Figure 4d, acquired at -100 °C, the signals remain stable for much higher doses ($>3.0 \times 10^{15} SF_5^+$ ions/cm²), enough so that the diffusion profile of the sirolimus in PLGA is clearly seen. The average crater depth obtained from the 50% sirolimus samples sputtered at low temperatures was $1.6 \mu m \pm 0.2 \mu m$, much thicker than at room temperature.

These experiments were also run using both Bi_1^+ and Ga^+ atomic primary ions under similar conditions in order to demonstrate the importance of using clusters for analysis. Figure 4e shows a representative profile of the 50% sirolimus formulation acquired using a Ga^+ primary ion source at -100 °C. Notice that the molecular signal obtained using Bi_3^+ is 10 times higher than that obtained with Ga^+ . More importantly, however, is the improvement in the overall quality of information obtained with Bi_3^+ , where the sirolimus signal indicates a very well-defined diffusion profile. This is not the case when using Ga^+ , most likely due to significant reductions in signal. Bi^+ depth profiles were similar to Ga^+ , but had higher signals than Ga^+ . Overall, there was increased damage accumulation occurring when using the

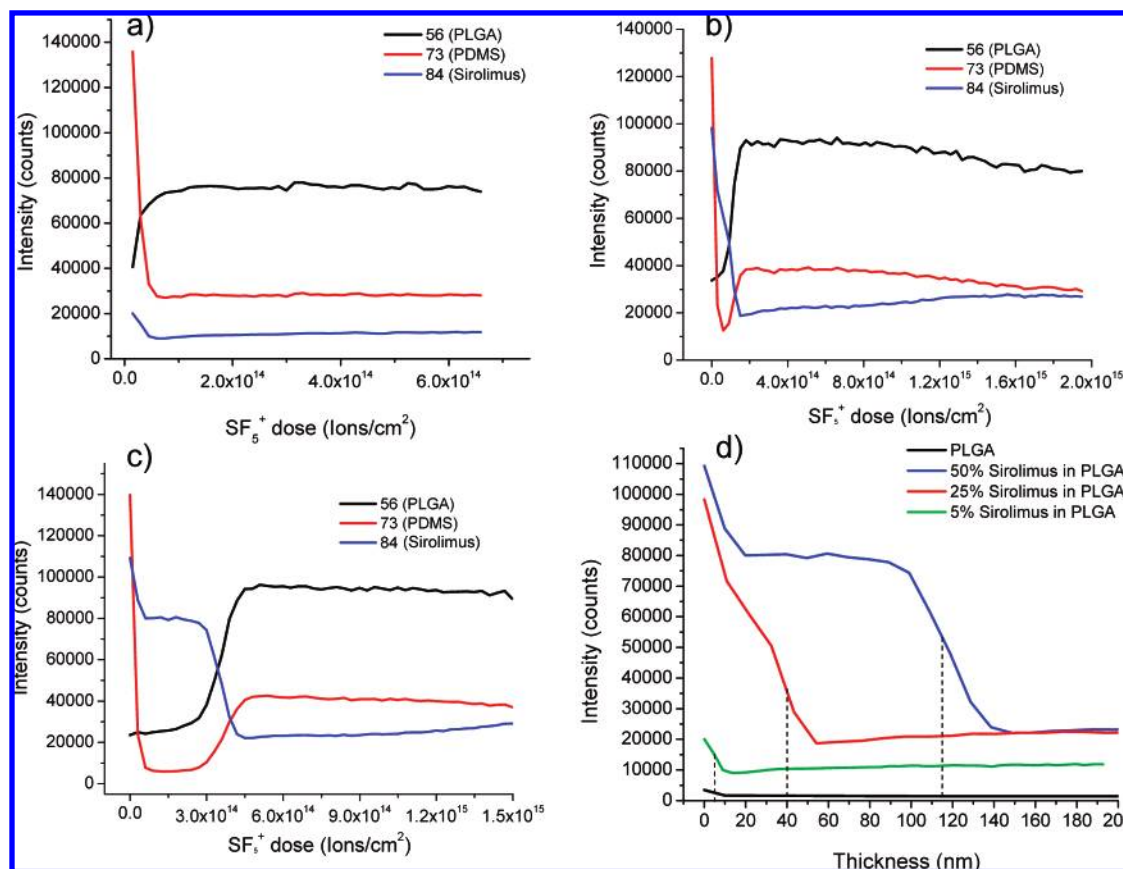


Figure 5. (a–c) Selected secondary ion intensities plotted as a function of ion dose for thick films on MP35N alloy coupons: (a) 5% sirolimus in PLGA, (b) 25% sirolimus in PLGA, and (c) 50% sirolimus in PLGA. (d) Actual depth profile overlays of $m/z = 84$ (sirolimus) at various concentrations. These plots were taken of the subsurface region only, with 2-s sputter intervals as opposed to 15 s in previous examples.

atomic beams for analysis (for both Bi^+ and Ga^+), resulting from the increased energy per unit impact.

Figure 5 shows depth profiles focusing only on the surface and subsurface region, as this is where the greatest intensity variations occur. In order to acquire these profiles, the sputter intervals were reduced (1 s–2 s) to maximize the number of data points in this region. Similar to what was observed in the thin model films, all concentrations exhibited a surface-enriched drug region, followed immediately by a drug-depletion zone and then a constant composition bulk region. There was also a significant amount of PDMS contaminant at the surface, which was removed with sputtering. Notice that the PDMS peak at $m/z = 73$ intensifies again in correspondence with the PLGA intensity. This increase results from an overlapping PLGA peak also located at a nominal mass of 73 Da ($C_3H_5O_2^+$). Other PDMS peaks (e.g., $m/z = 147$, 201, and 221) do not increase at this point.

From these plots, one can determine the thickness of the drug overlayer and relate it to the performance characteristics of the device. This was done by taking the derivative plots of both $m/z = 84$ and $m/z = 56$ plotted on a depth scale. The average overlayer thickness based on at least three samples per concentration turned out to be $4.5 \text{ nm} \pm 0.04 \text{ nm}$ for the 5% sirolimus film, $46.2 \text{ nm} \pm 10.0 \text{ nm}$ for the 25% sirolimus film, and $123.8 \text{ nm} \pm 34.0 \text{ nm}$ for the 50% sirolimus film. It can be seen that for this system, as the drug concentration increases, the thickness of the drug-rich region increases as well. At 50% sirolimus, there is a very stable plateau region.

3-D Images. One of the most exciting aspects of utilizing cluster primary ions for organic applications is the ability to obtain 3-D information, where images can be reconstructed from the raw data files to obtain 3-D molecular compositional information about the films and relate this structure to the release characteristics. An example is illustrated in Figure 6, which depicts the 3-D structure in a 25% sirolimus sample. In this example, the ion maps of sirolimus ($m/z = 84$) and PLGA ($m/z = 99$, $C_5H_7O_2^+$) are plotted as a function of increasing depth into the sample. Also shown is an overlay map of both ions as a function of depth. In this particular film, the surface is composed mostly of drug. However, after sputtering, PLGA domains are revealed, which increase in size up through to the bulk region. At this point ($\sim 65 \text{ nm}$), drug-rich particulate features are observed in a PLGA matrix. The 50% sample had a very similar 3-D structure (not shown) in that there were PLGA domains present below the surface, though with much less PLGA in the subsurface region and a thicker drug overlayer. The 5% film was completely homogeneous throughout the film, with higher average drug signals originating from the surface than in the bulk (data not shown). All of these results are consistent with the 3-D structure as determined by other methods, such as confocal Raman microscopy.²⁰

Drug-Eluting Stents. The capabilities of cluster SIMS for depth profiling in polymeric drug delivery systems indicate that it is a useful tool to elucidate the 3-D structure in these complicated systems. However, these thick films on metal still represent a model system for DES. Actual DES have much more

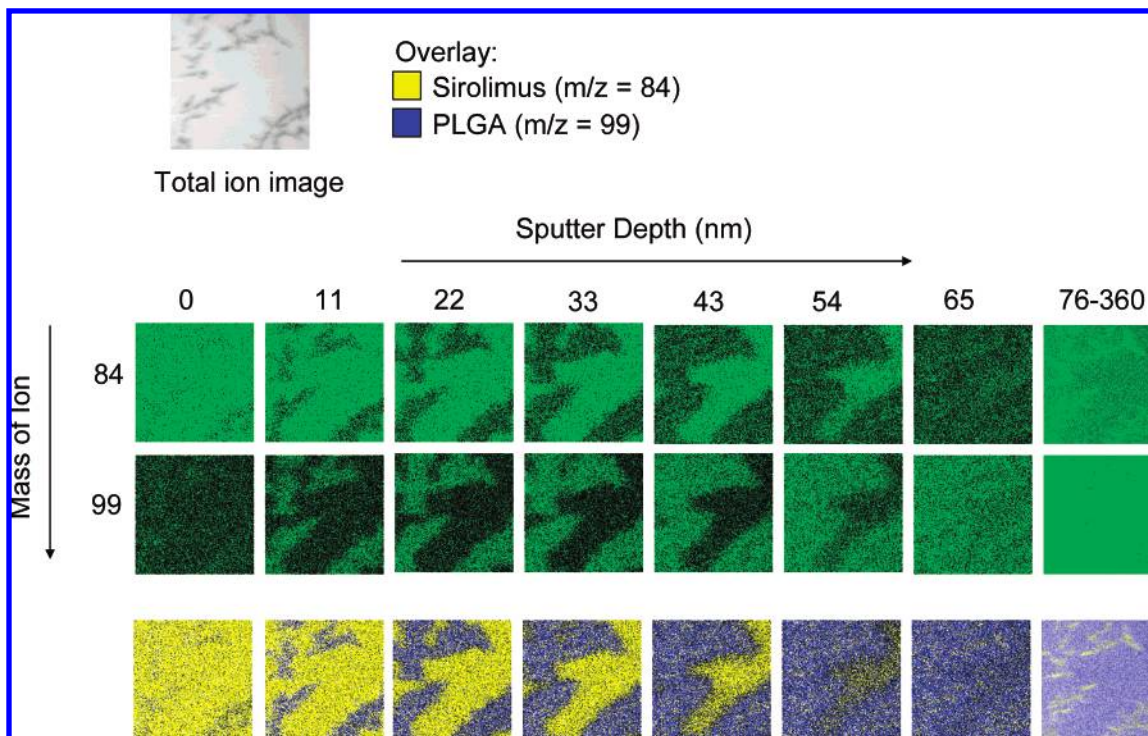


Figure 6. 3-D mapping ($300\ \mu\text{m} \times 300\ \mu\text{m}$) of the distribution of drug and polymer in a DES system containing 25% sirolimus in PLGA. Signals monitored were $m/z = 84$ (sirolimus) and $m/z = 99$ (PLGA). Blue and yellow images represent an overlay of both components. The total ion image is shown in the top left-hand corner and represents the sum of all secondary ion signals from a given area.

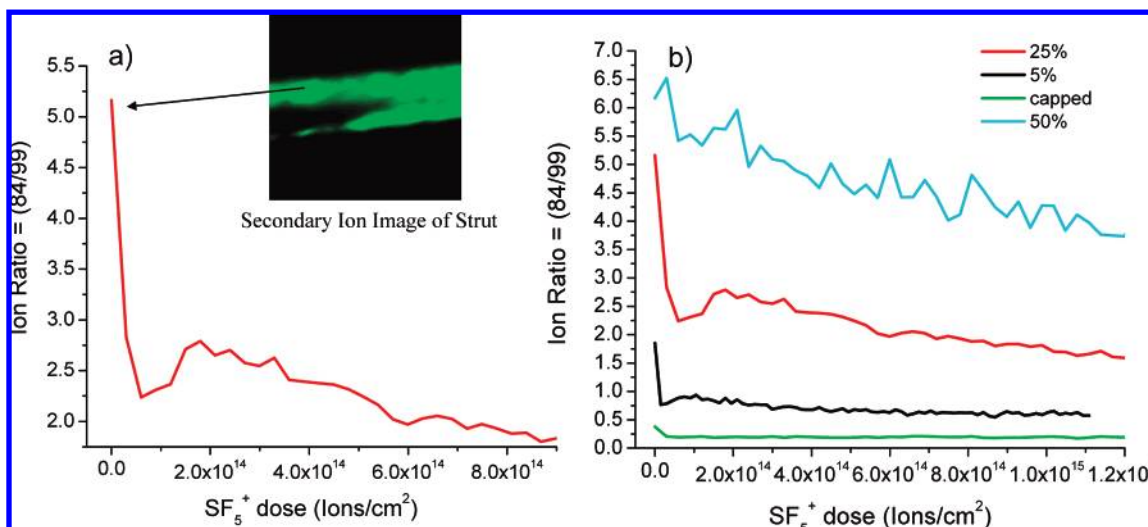


Figure 7. Plots of intensity ratios of $m/z = 84$ (drug) to $m/z = 99$ (polymer) as a function of increasing SF_5^+ dose in drug-eluting coronary stents: (a) 25% sirolimus in PLGA. For all profiles, the signal was selected only from the stent (see green areas in image). (b) Overlay of coronary stents of varying sirolimus concentrations. A capped sample is included. All stents were analyzed at $-100\ ^\circ\text{C}$

complicated geometries, which can be difficult when SIMS analysis is being performed. Figure 7 shows representative profiles of the surface region on a stent spray coated with a film of 25% sirolimus in PLGA, acquired at $-100\ ^\circ\text{C}$. The results indicate that, although it is difficult, SIMS can be used to characterize the surface and in-depth distribution of a drug in stent coatings, though manipulation of the raw data is required to account for spectral shifts within the rastered area and for unoptimized beam geometries (i.e., sputter gun is on opposite side of analysis gun). After taking a ratio of the sirolimus signal ($m/z = 84$) to that of the PLGA signal ($m/z = 99$), and extracting data only from the region of interest (e.g., the stent, and not the background), we

could obtain useful information about the distribution of the drug in the film, where a typical diffusion profile of the drug is obtained, consistent with what was observed in the coupons.

Figure 7b shows an overlay of the depth profiles that were acquired from stents of varying compositions. Also included here is a “capped” sample. This sample was created by spray coating a 25% sirolimus coating ($\sim 3.5\ \mu\text{m}$) onto the stent, followed by spray coating another layer of pure PLGA ($\sim 3.5\ \mu\text{m}$) on top of the previous layer. This type of procedure is often done in stents to prevent initial burst release effects that may occur. The 5% and 25% samples display the same characteristic diffusion profiles as was observed in the coupons. However, the 50% sample is difficult

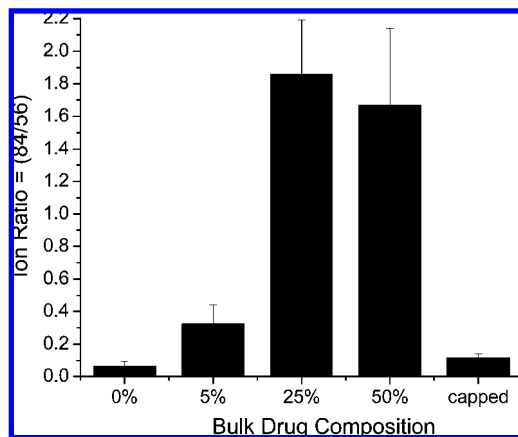


Figure 8. Ratio at the surface of $m/z = 84$ (drug) to $m/z = 56$ (polymer) plotted as a function of increasing drug composition. A capped sample is included.

to interpret at this point. This could be because the overlayer thickness is too great, or it could be because there is nonuniform sputtering resulting in increased damage.

While depth profiling did prove difficult, surface analysis was a much easier process with very informative results. Figure 8 plots the ratio of $m/z = 84$ (sirolimus) to $m/z = 56$ (PLGA) as a function of bulk composition. The control sample (PLGA alone) has a very low ratio. The intensity ratio then increases from 5% to 25% as is expected. The intensity ratio of the 50% sample is similar to the 25% sample (also observed in the coupons). Also included here is the capped sample. As can be seen, the intensity ratio of the capped sample is very low and is not significantly different from that of the control sample of 100% PLGA, indicating that there is no detectable diffusion of the drug to the surface in this sample.

CONCLUSIONS

Cluster primary ion sources were used to obtain three-dimensional molecular information from drug-eluting stent coatings of varying compositions. It was determined for all composi-

tions that the drug tended to diffuse to the surface, forming a characteristic diffusion profile. This diffusion profile is defined by a drug-enriched surface region, followed immediately by a drug depletion region and, finally, a constant bulk composition region. In these depth profiles, it was observed that the overlayer thickness increased with increasing drug content.

3-D molecular information was reconstructed from the raw data files, where it was determined that the 5% samples were quite homogeneous on a lateral scale. However, both the 25% and 50% samples displayed domain formation in the surface, near-surface, and bulk regions.

Finally, though it was proven to be difficult due to complications in geometry, molecular depth profiling of coatings on stents is feasible. The diffusion profiles acquired from the films coated onto stents appeared to be very similar to that obtained for the coupons.

The importance of temperature on depth profiling in these systems was also demonstrated, where it was determined that, for all compositions, low temperatures yielded optimum results. This was attributed to decreased topography formation at low temperatures as a result of more uniform sputtering.

These results clearly demonstrate the utility of cluster SIMS as a tool for characterization of drug-eluting stent coatings but also show promise for other polymeric based drug delivery devices, biomaterials, or both. The 3-D molecular compositional information obtained using cluster SIMS will be useful for predicting, optimizing, and verifying the performance characteristics in many drug delivery devices.

ACKNOWLEDGMENT

We would like to thank Phillip McDonald and Chris Hobot (both of Medtronic) for preparation of the coated stents and coupons.

Received for review August 2, 2007. Accepted October 5, 2007.

AC701644J